DALTON
FULL PAPER

Hole states in $Eu_{0.9-x}Pr_xCa_{0.1}BaSrCu_3O_{7-\delta}$ studied by X-ray absorption spectroscopy

Ponnusamy Nachimuthu,[a] Jin-Ming Chen,[b] Ru-Shi Liu,[a] Tryambak Bhimsen Waje,[c] Iyyani Kunjappu Gopalakrishnan[d] and Jatinder Vir Yakhmi[d]

[a] *Department of Chemistry, National Taiwan University, Taipei, Taiwan, ROC*
[b] *Synchrotron Radiation Research Center, Hscinchu, Taiwan, ROC*
[c] *Computer Division, Bhabha Atomic Research Center, Mumbai 400 085, India*
[d] *Chemistry Division, Bhabha Atomic Research Center, Mumbai 400 085, India*

Received 5th October 1998, Accepted 15th April 1999

The hole states located on different oxygen sites have been investigated in $Eu_{0.9-x}Pr_xCa_{0.1}BaSrCu_3O_{7-\delta}$ with increasing Pr^{3+} substitution by high-resolution oxygen K-edge and copper L-edge X-ray absorption spectra. The results reveal that the hole states are depleted systematically by the substitution and in turn lead to a reduction in T_c. However, the rate at which the depletion occurs is lower in $Eu_{0.9-x}Pr_xCa_{0.1}BaSrCu_3O_{7-\delta}$ compared to that in $Y_{1-x}Pr_xBa_2Cu_3O_{7-\delta}$ and $Dy_{1-x}Pr_xBa_2Cu_3O_{7-\delta}$. This is due to the partial substitution of Ba^{2+} by Sr^{2+} ions and R (rare earth element) by Ca^{2+} ions in the present case. The depletion of hole states gives evidence in support of the hole-depletion models based on Pr 4f–O $2p_\pi$ hybridization. The possible reasons for the anomalous behavior of Pr^{3+} ions in $RBa_2Cu_3O_{7-\delta}$ are also discussed.

Introduction

The materials $RBa_2Cu_3O_{7-\delta}$ (R123) where R = rare earth element, are known to show a superconducting transition temperature (T_c) above 90 K except where R = Ce, Pr or Tb.[1,2] Though isomorphic structure is not formed where R = Ce or Tb unlike the other rare earth based R123 compounds,[2] ideal orthorhombic structure similar to that of other superconducting R123 compounds is formed but no superconductivity is exhibited by $PrBa_2Cu_3O_{7-\delta}$ (Pr123).[3–9] This anomalous behavior of $PrBa_2Cu_3O_{7-\delta}$ is not fully understood although much has been published about the aspects related to non-superconducting nature of this compound.[3–9] Recently, there have been some reports suggesting superconductivity in Pr123 but these have met with considerable skepticism owing to the lack of reproducibility of data and the existence of an anomalously long *c* axis reported for the structure of Pr123.[6,10–15]

Several models have been proposed during the past few years to explain the anomalous behavior of $PrBa_2Cu_3O_{7-\delta}$.[3] The most widely discussed deal with the hole filling[16–18] or pair breaking mediated by the hybridization of praseodymium 4f and oxygen 2p states of the CuO_2 planes.[19] The hole filling model assumes that Pr has a valence of more than +3 whereby the extra electrons from Pr neutralize the mobile holes which in turn brings the compound to a near insulating regime. However, this model has not met with great success since a valence exceeding +3 for Pr is not supported by many experimental findings.[20–24] On the other hand, pair breaking appeared to be a more promising model as it can explain the suppression of superconductivity in $R_{1-x}Pr_xBa_2Cu_3O_{7-\delta}$ through the hybridization of praseodymium 4f and oxygen 2p states of the CuO_2 planes leading to the localization of the holes, although pair breaking by itself cannot account for the insulating behavior of $PrBa_2Cu_3O_{7-\delta}$.[19] Recently, two models have been proposed by Fehrenbacher and Rice (FR)[25] and Liechtenstein and Mazin (LM),[26] both of which involve the transfer of holes from the pd_σ state to the pd_π state. In the FR model the $4f_{z(x^2-y^2)}$ orbital of Pr^{3+} ion is hybridized with p_π orbitals of neighboring planar oxide ions. The p_π holes are treated as planar (p_{xy}) in the FR model, whereas they have comparable amounts of $p_{x,y}$ and p_z character in the LM model. These models are well supported by a polarization dependent X-ray absorption study on detwinned $Y_{1-x}Pr_xBa_2Cu_3O_{7-\delta}$ single crystals.[7] Although both FR and LM models can explain the insulating behavior of $PrBa_2Cu_3O_{7-\delta}$, they do not account for a high value of nearly 17 K for the antiferromagnetic ordering of praseodymium moments (Neel temperature T_N) for this compound.[6,9]

Earlier experimental reports have demonstrated that the hole states play a vital role in superconductivity in the p-type cuprate superconductors. Therefore, knowledge of the electronic structure near the Fermi level of these compounds is important to understand the mechanism of superconductivity. The X-ray absorption spectra are determined by electronic transitions from a selected atomic core level to the unoccupied electronic states near the Fermi level. X-Ray absorption near edge structure (XANES) is therefore a direct probe of the character and local density of the hole states responsible for the high temperature superconductivity. It has been generally accepted that the hole states in p-type cuprate superconductors are located on oxygen sites. Moreover, there are several non-equivalent oxygen sites in these materials. Therefore it becomes necessary to understand the distribution of hole states among different oxygen sites and their role in superconductivity as well.

The recent works on bulk and thin films of $PrBa_{2-x}Sr_xCu_3O_{7-\delta}$ show that strontium doping at the barium site increases the distance between Pr^{3+} and O^{2-} ions in the CuO_2 plane and consequently leads to a dramatic decrease of resistivity in doped samples.[9] Very recently, Liu *et al.*[5] also suggested in support of the above observations that chemical substitution of Sr for Ba in $YBa_{2-x}Sr_xCu_3O_{7-\delta}$ gives rise to higher hole concentrations, leading to an overdoped state. As a result, a decrease in T_c was found from 92 K when $x = 0.0$ to 84 K when $x = 0.8$, which was the maximum solubility of Sr without modifying the phase. Similarly, the holes induced by the Ca^{2+} ions in $Pr_{0.5}Ca_{0.5}Ba_2Cu_3O_{7-\delta}$ thin films lead to the recovery of the high temperature superconductivity for the Pr123 phase.[14] Recently, this was also well brought out by Merz *et al.*[8] based on their polarization dependent X-ray absorption spectral studies on $Y_{1-x}Ca_xBa_2Cu_3O_{7-\delta}$ single crystals. They found that the maximum hole counts correspond to the composition

$Y_{0.9}Ca_{0.1}Ba_2Cu_3O_{6.91}$. All these reports clearly indicate that the substitution of Ba^{2+} partially by Sr^{2+} ions and R by Ca^{2+} ions induces and creates the holes, in contrast to the substitution of Pr^{3+} ions at the R site which always depletes the hole content. In addition, it has been reported that $Eu_{1-x}Pr_xBa_2Cu_3O_{7-\delta}$ becomes an insulator when $x \geq 0.5$. However, $Eu_{1-x}Pr_xBaSrCu_3O_{7-\delta}$ and $Eu_{0.9-x}Pr_xCa_{0.1}BaSrCu_3O_{7-\delta}$ do show superconductivity unlike $Eu_{1-x}Pr_xBa_2Cu_3O_{7-\delta}$ even when $x = 0.5$ (Table 1). X-Ray absorption studies on $Y_{1-x}Pr_xBa_2Cu_3O_{7-\delta}$ and $Dy_{1-x}Pr_xBa_2Cu_3O_{7-\delta}$ indicate that the depression of T_c is due to the depletion of the hole states by Pr^{3+} substitution and the rate at which the depletion occurs is comparable for both systems.[4,7] However, there has been no report of X-ray absorption spectroscopy on R123 by substituting Ba^{2+} partially by Sr^{2+} ions and R by Ca^{2+} and Pr^{3+} ions. Therefore, we have chosen a series of compounds corresponding to the composition $Eu_{0.9-x}Pr_xCa_{0.1}BaSrCu_3O_{7-\delta}$, where $x = 0.1$–0.5, for the present study. Preliminary data for the present and the related systems, *viz.* $Eu_{1-x}Pr_xBa_2Cu_3O_{7-\delta}$ and $Eu_{1-x}Pr_xBaSrCu_3O_{7-\delta}$ where $x = 0.0$–0.5, have been reported elsewhere.[27,28] The corresponding T_c values are reproduced in Table 1. It has been shown in the present study that the hole states are depleted systematically which in turn leads to reduction in T_c by the substitution of Pr^{3+} ions in $Eu_{0.9-x}Pr_xCa_{0.1}BaSrCu_3O_{7-\delta}$. However, the rate at which the depletion occurs is lower when compared to those of the $Y_{1-x}Pr_xBa_2Cu_3O_{7-\delta}$ and $Dy_{1-x}Pr_xBa_2Cu_3O_{7-\delta}$ systems.

Table 1 The T_c values for $Eu_{1-x}Pr_xBa_2Cu_3O_{7-\delta}$, $Eu_{1-x}Pr_xBaSrCu_3O_{7-\delta}$ and $Eu_{0.9-x}Pr_xCa_{0.1}BaSrCu_3O_{7-\delta}$, and the oxygen contents $(7-\delta)$ for $Eu_{0.9-x}Pr_xCa_{0.1}BaSrCu_3O_{7-\delta}$

	T_c/K ± 1					
Composition	x 0.0	0.1	0.2	0.3	0 .4	0.5
$Eu_{1-x}Pr_xBa_2Cu_3O_{7-\delta}$	94.8	79.5	57.9	38.8	15.0	0.0
$Eu_{1-x}Pr_xBaSrCu_3O_{7-\delta}$	84.0	68.0	62.0	53.0	37.5	26.7
$Eu_{0.9-x}Pr_xCa_{0.1}BaSrCu_3O_{7-\delta}$	77.0	69.0	65.0	60.0	33.7	21.4
	Oxygen content $(7-\delta)$ ± 0.02					
$Eu_{0.9-x}Pr_xCa_{0.1}BaSrCu_3O_{7-\delta}$	—	6.95	6.97	6.98	6.97	6.99

Experimental

The samples $Eu_{0.9-x}Pr_xCa_{0.1}BaSrCu_3O_{7-\delta}$ ($x = 0.1$, 0.2, 0.3, 0.4 or 0.5) were prepared by solid state reactions of the respective oxides or nitrates at 1250 K. Stoichiometric amounts of Eu_2O_3, Pr_6O_{11}, $Ba(NO_3)_2$, $Sr(NO_3)_2$, $CaCO_3$ and CuO obtained from Aldrich Chem. Co. (99.9%) were weighed and mixed thoroughly in an agate pestle and mortar. The mixtures were then transferred to a platinum crucible and placed in a furnace. Initially the mixture was calcined at 1225 K for 24 h. The mixture was then pressed into pellets and sintered at 1250 K for 78 h. The heat treatment was interrupted every 24 h for grinding and pelletizations. The sintered samples were then annealed in flowing argon gas for 12 h at 1100 K, the furnace was cooled to 725 K and reannealed in oxygen for 72 h. The samples were then cooled to room temperature at the rate of 1 °C min^{-1}. The powder X-ray diffractograms were recorded on a Philips X-ray diffractometer (Model PW 1071) with nickel filtered Cu-Kα radiation. The analyses of powder X-ray diffractograms showed that all the samples were single phase. Iodometric titration was used to determine the oxygen contents for the samples.[28] The T_c values were obtained for the above compounds by using an APD cryocooler with a Meissner coil attachment in conjunction with an E.G. and G.P.A.R. two-phase lock-in amplifier (Model 5280).

The X-ray absorption measurements for the polycrystalline samples were carried out at the 6 m high energy spherical grating monochromator (HSGM) beam line of the Synchrotron Radiation Research Center (SRRC), Taiwan, ROC with an electron beam energy of 1.5 GeV and a maximum stored current of 240 mA. The X-ray fluorescence yield (XFY) technique was adopted for recording the spectra by using a micro channel plate (MCP) as a detector. The MCP detector is composed of a dual set of micro channel plates with an electrically isolated grid mounted in front of them. The X-ray fluorescence yield technique is strictly bulk sensitive with a probing depth of thousands of angstroms in contrast to the electron yield technique. During the X-ray fluorescence yield measurements the grid was set to a voltage of 100 V, while the front of the MCP was set at −2000 V and the rear at −200 V. The grid bias insured that positive ions would not be detected while the MCP bias insured that no electrons were detected. The MCP detector was located at ≈2 cm from the sample and oriented parallel to the sample surface. The photons were incident at an angle of 45° with respect to the sample normal. The incident photon intensity (I_0) was monitored simultaneously by a nickel mesh located after the exit slit of the monochromator. All the measurements were normalized to I_0. The photon energies were calibrated using the known oxygen K-edge and copper L_3-edge absorption peaks of CuO. The energy resolution of the monochromator was set to ≈0.22 and ≈0.45 eV for the oxygen K-edge and copper L_3-edge X-ray absorption spectral measurements, respectively. All the measurements were performed at room temperature.

Results and discussion

The oxygen contents of $Eu_{0.9-x}Pr_xCa_{0.1}BaSrCu_3O_{7-\delta}$ where $x = 0.1$, 0.2, 0.3, 0.4 or 0.5 as determined by the iodometric titrations are given in Table 1. These values remain unaltered at ≈6.97 ± 0.02 with increasing praseodymium substitution, indicating that Pr is in trivalent state and is substituting at the europium site. The ionic size of Ca^{2+} is closer to that of Eu^{3+} ion, rather than that of Ba^{2+}/Sr^{2+},[30] but its valence would favor its going to the Ba/Sr site. However, an earlier study on $Eu_{1-x}Ca_xBaSrCu_3O_{7-\delta}$ by Waje *et al.*[31] found that the lattice parameter '*a*' increased with increasing calcium concentration '*x*' indicating that Ca substitutes at the europium site.

The oxygen K-edge X-ray absorption spectra of $Eu_{0.9-x}Pr_xCa_{0.1}BaSrCu_3O_{7-\delta}$ where $x = 0.1$, 0.2, 0.3, 0.4 or 0.5 obtained by the X-ray fluorescence yield technique are shown in Fig. 1. All these spectra were normalized to their respective absorption cross-sections of the actual oxygen contents given in Table 1. The salient features of these spectra are as follows. There are two prepeaks at ≈528.3 and ≈529.4 eV with a shoulder at 527.5 eV, and a broad peak at ≈537 eV. The low-energy transitions with energy below 532 eV are ascribed to transitions from the oxygen 1s core electrons to holes with predominant 2p character on the oxygen sites. The transitions with energy above 532 eV are attributed to the transitions to oxygen 2p states, which are hybridized with barium-4d, strontium-3d, praseodymium-5d or 4f states.[24]

The system $Eu_{0.9-x}Pr_xCa_{0.1}BaSrCu_3O_{7-\delta}$ is isomorphic with $YBa_2Cu_3O_{7-\delta}$ (orthorhombic structure with space group *pmmm*) at lower Pr^{3+} concentrations. However, with increasing Pr^{3+} concentration, *i.e.* when $x = 0.3$ and above, the phase changes from orthorhombic structure to tetragonal structure.[27,28] The tetragonal structure is again isomorphic with $YBa_2Cu_3O_6$.[32] We therefore adopted the same scheme of assignments for the present oxygen 1s absorption spectra as the samples belong to both orthorhombic as well as tetragonal phases. A study on $R(Ba_{1-z}R_z)_2Cu_3O_{7-\delta}$ (R = Nd or Pr) by soft X-ray absorption spectroscopy also supports the present assignments.[33] The orthorhombic crystal structure of $Eu_{0.9-x}Pr_xCa_{0.1}BaSrCu_3O_{7-\delta}$ has four non-equivalent oxygen sites, *viz.* O(2) and O(3) within the Cu(2)O_2 layers, O(4) in the BaO and SrO planes, and O(1) in the Cu(1)O chains along the *b* axis.

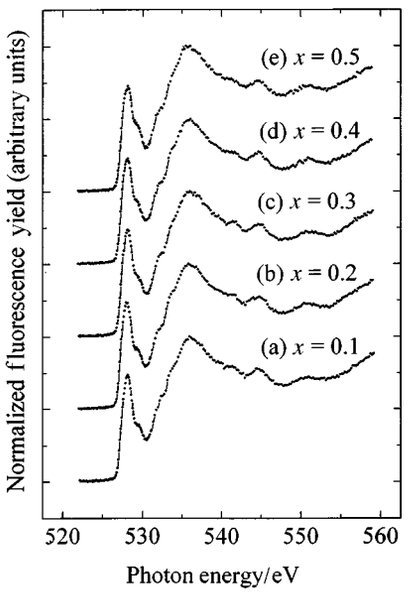

Fig. 1 Oxygen K-edge X-ray absorption spectra for $Eu_{0.9-x}Pr_x$-$Ca_{0.1}BaSrCu_3O_{7-\delta}$. All these spectra were normalized to their respective absorption cross-sections of the actual oxygen contents given in Table 1.

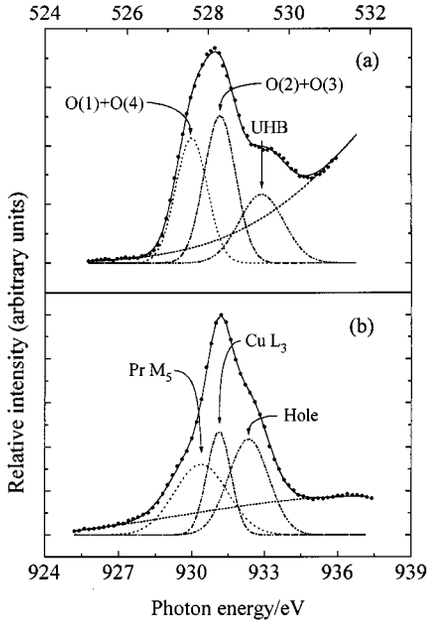

Fig. 2 Pre-edge structure of the oxygen K-edge (a) and copper L_3-edge (b) X-ray absorption spectra for $Eu_{0.8}Pr_{0.1}Ca_{0.1}BaSrCu_3O_{7-\delta}$. The dashed lines represent the resolved Gaussian components of the spectra. ●, Experimental; ——, fit.

The observed multiple transitions at energy below 532 eV are related to the chemical shifts of oxygen 1s binding energies for different oxygen sites. The differences in the chemical shifts of oxygen 1s core levels can be obtained by using local density approximation (LDA) band-structure calculations. Based on LDA calculations for $YBa_2Cu_3O_{7-\delta}$ by Krakauer *et al.*,[34] the oxygen 1s energy levels of the sites O(2) and O(3) in the $Cu(2)O_2$ planes were very close to each other and found to be 0.29 eV higher than that of the O(1) site in the Cu(1)O chains which in turn was 0.4 eV higher than the energy level of the O(4) site in the BaO planes. Based on these LDA calculations and earlier reports on isomorphic systems, *viz.* $YBa_2Cu_3O_{7-\delta}$, $PrBa_2Cu_3O_{7-\delta}$ and $DyBa_2Cu_3O_{7-\delta}$, the following assignment scheme for the oxygen 1s absorption spectra of $Eu_{0.9-x}Pr_xCa_{0.1}BaSrCu_3O_{7-\delta}$ is made.[4,7,8,24,34–37] The shoulder at 527.5 eV is assigned to the transition from the oxygen 1s core level to the superposition of oxygen 2p hole states originating from the apical oxygen sites, *viz.* O(4) sites in the BaO and SrO planes, and oxygen sites in Cu(1)O chains, *viz.* O(1). The high energy prepeak at 528.3 eV is due to the transition into oxygen 2p holes on O(2) and O(3) sites situated in the $Cu(2)O_2$ planes. The peak at 529.4 eV is ascribed to the transition into the conduction band, in other words the upper Hubbard band (UHB) which is predominantly formed by copper 3d states with some admixture of oxygen 2p states.[38,39] As a consequence of the strong on-site correlation effects on the copper sites in cuprate superconductors, the upper Hubbard band is always assumed to be present.[40] The spectral weight of the component corresponding to the transition to the hole states on O(2) and O(3) sites situated in $Cu(2)O_2$ planes decreases, while the component corresponding to the transition to the upper Hubbard band increases, with increasing Pr^{3+} substitution for Eu^{3+} in $Eu_{0.9-x}$-$Pr_xCa_{0.1}BaSrCu_3O_{7-\delta}$ (Fig. 1). These observations clearly demonstrate that the chemical substitution of Pr^{3+} for Eu^{3+} in $Eu_{0.9-x}Pr_xCa_{0.1}BaSrCu_3O_{7-\delta}$ reduces the hole states in $Cu(2)O_2$ planes.

To estimate the hole states on different oxygen sites and to understand the variation of hole states for different praseodymium substitution, the oxygen K-edge X-ray absorption spectra as shown in Fig. 1 were resolved into different Gaussian components by the following procedure. By fixing the band positions obtained by plotting the second derivative form, the bandwidths were evaluated over a series. It was found that the

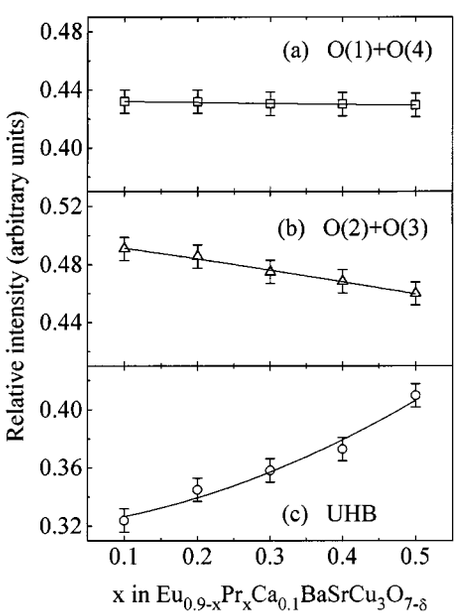

Fig. 3 Plots of the relative intensities of hole states in $Eu_{0.9-x}Pr_x$-$Ca_{0.1}BaSrCu_3O_{7-\delta}$ on oxygen sites originating from the (a) CuO_3 ribbons, (b) CuO_2 planes and (c) the upper Hubbard band (UHB) as a function of Pr^{3+} substitution. The solid lines are guides to the eyes.

bandwidths obtained from the fits were almost constant for a particular band over a series. These bandwidths were averaged over a series for a particular band. Then the resultant bandwidths were fixed for the final fit and the band positions allowed to vary. The goodness of fit was judged by the χ^2 value. The relative intensities of each Gaussian component were obtained by integrating the area under the band. The errors in the relative intensities of each Gaussian component were obtained as standard errors (the square root of the mean square error) for the best fits. As an illustrative example, the pre-edge structure of oxygen 1s X-ray absorption spectrum of $Eu_{0.8}Pr_{0.1}Ca_{0.1}BaSr$-$Cu_3O_{7-\delta}$ including the Gaussian components along with their assignments is shown in Fig. 2(a). The resultant spectral weights for different Gaussian components are plotted as a function of praseodymium substitution in Fig. 3. All these spectral weights were normalized to that of the intense band at

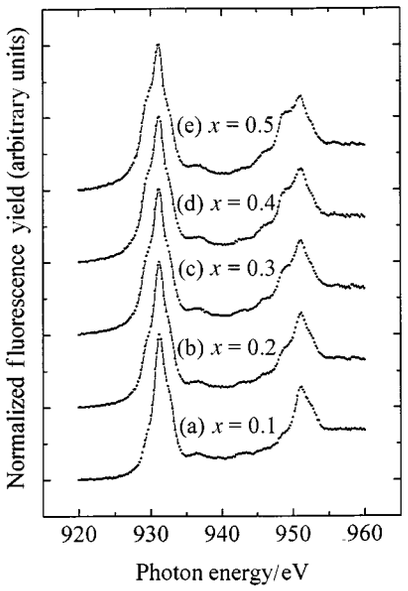

Fig. 4 Praseodymium M_{45}-edge and copper L_{23}-edge X-ray absorption spectra for $Eu_{0.9-x}Pr_xCa_{0.1}BaSrCu_3O_{7-\delta}$.

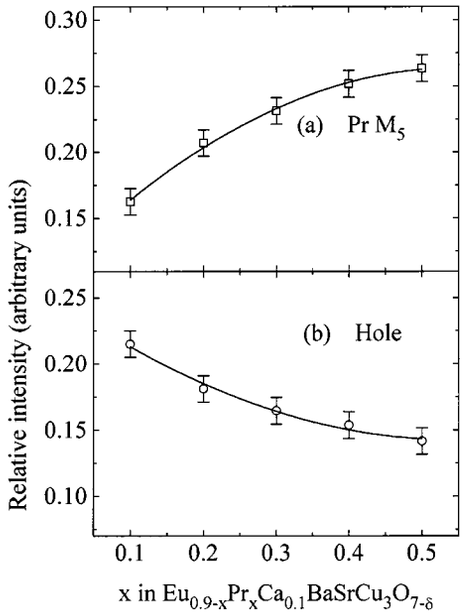

Fig. 5 Plots of the relative intensities of (a) the band at ≈930 eV originating from $3d_{5/2}$ to 4f of Pr^{3+} and (b) the defect state at ≈932 eV on the copper sites, for $Eu_{0.9-x}Pr_xCa_{0.1}BaSrCu_3O_{7-\delta}$ as a function of Pr^{3+} substitution. The solid lines are guides to the eyes.

≈537 eV. The spectral weight at 527.5 eV corresponding to oxygen 2p hole states on the apical oxygen sites, *viz.* O(4), and on the Cu(1)O chains, *viz.* O(1), is constant with increasing praseodymium substitution (Fig. 3). On the other hand, the spectral weight at 528.3 eV corresponding to oxygen 2p hole states on the O(2) and O(3) sites situated in the $Cu(2)O_2$ planes decreases systematically, while the spectral weight of the upper Hubbard band at 529.4 eV is found to increase at the cost of hole states on the O(2) and O(3) sites in the $Cu(2)O_2$ planes with increasing praseodymium substitution (Fig. 3).

The praseodymium M_{45}-edge and copper L_{23}-edge X-ray absorption spectra of $Eu_{0.9-x}Pr_xCa_{0.1}BaSrCu_3O_{7-\delta}$ where $x = 0.1$, 0.2, 0.3, 0.4 or 0.5 obtained by the X-ray fluorescence yield technique are shown in Fig. 4. The bands centered at ≈931 and ≈951 eV are called copper L_3 and L_2 white lines, and are assigned to the transitions from the ground states of Cu^{2+}, $Cu(2p_{3/2,1/2})3d^9$–O $2p^6$, into the excited states, $Cu(2p_{3/2,1/2})^{-1}3d^{10}$–O $2p^6$, respectively, where $(2p_{3/2,1/2})^{-1}$ denotes a hole containing $2p_{3/2}$ or $2p_{1/2}$ states.[41,42] The shoulders situated to high energy of each main band are assigned to the transitions from the ground states of Cu^{3+}, $Cu(2p_{3/2,1/2})3d^9L^{-1}$ into the excited states, $Cu(2p_{3/2,1/2})^{-1}3d^{10}L^{-1}$, respectively, where L^{-1} denotes a ligand hole on the oxygen 2p orbital. These high-energy shoulders are therefore identified as the holes in the CuO_2 layers and CuO_3 ribbons.[41,42] The shoulders to low energy of both copper L-edges are due to praseodymium M_5 and M_4 white lines respectively and are assigned to the transitions from $3d_{5/2}$ electrons to 4f states of Pr^{3+}. Attempts were made to resolve the copper L_3-edge and praseodymium M_5-edge X-ray absorption spectra and as a representative example the results of the spectrum corresponding to the composition $Eu_{0.8}Pr_{0.1}Ca_{0.1}BaSrCu_3O_{7-\delta}$ including the resolved Gaussian components and their assignments are shown in Fig. 2(b). The resultant spectral weights for Gaussian components corresponding to the transitions, *viz.* the hole contents in the CuO_2 layers and CuO_3 ribbons, and praseodymium M_5 white line, are plotted as a function of praseodymium substitution in Fig. 5. All these spectral weights are normalized to that corresponding to the transition due to Cu^{2+} at ≈931 eV. The spectral weight corresponding to the total hole contents decreases while that corresponding to the praseodymium M_5 white line increases with increasing praseodymium concentration. The increase in the spectral weight corresponding to the M_5 white line confirms that Eu^{3+} ions in the $Eu_{0.9-x}Pr_xCa_{0.1}BaSrCu_3O_{7-\delta}$ system are partially substituted by Pr^{3+} ions. The decrease in hole content with increasing Pr^{3+} is also evidenced by the oxygen K-edge X-ray absorption spectra as discussed earlier.

The present experimental results based on oxygen K-edge and copper L-edge X-ray absorption spectra for $Eu_{0.9-x}Pr_xCa_{0.1}BaSrCu_3O_{7-\delta}$ clearly demonstrate that the hole states responsible for superconductivity get depleted progressively by the praseodymium substitution.[43] These should in principle reduce the T_c, which is indeed found to be the case. Thus these results give evidence in support of the hole-depletion models based on Pr 4f–O $2p_\pi$ hybridization.[25,26] By comparing the depletion of hole states upon praseodymium substitution in $Eu_{0.9-x}Pr_xCa_{0.1}BaSrCu_3O_{7-\delta}$ with those in $Y_{1-x}Pr_xBa_2Cu_3O_{7-\delta}$ and $Dy_{1-x}Pr_xBa_2Cu_3O_{7-\delta}$, it is found that the rate at which the depletion of hole states occurs in the present case is lower than in $Y_{1-x}Pr_xBa_2Cu_3O_{7-\delta}$ and $Dy_{1-x}Pr_xBa_2Cu_3O_{7-\delta}$.[4,7] This is due to the partial substitution of Ba^{2+} by Sr^{2+} and Eu by Ca^{2+} ions which keeps inducing and creating the holes which in turn leads to a decrease in the rate of hole depletion in the present case.

It is well known that the phenomenological Judd–Ofelt model can account for the observed intensities for 4f–4f transitions of all the rare earth ions except Pr^{3+}.[44–46] In the case of Pr^{3+} ions, the 5d level is relatively low lying which results in a strong mixing with the 4f orbital. This is reflected by the abnormal intensity reported for the transition $^3H_4 \longrightarrow {}^3P_2$ in the absorption spectra measured in the uv-visible region for Pr^{3+} ion in different host materials.[44–46] The models proposed by FR and LM consider that the $4f_{z(x^2-y^2)}$ orbital of Pr^{3+} is strongly localized and hybridized with p_π orbitals of neighboring planar oxide ions.[25,26] These models do not consider 4f–5d mixing for Pr^{3+} ion. The abnormal intensity reported for the transition $^3H_4 \longrightarrow {}^3P_2$ and the non-applicability of Judd–Ofelt theory for the Pr^{3+} ions suggest that the 4f orbital is strongly perturbed by the 5d orbital. One should take this effect into account when the 4f orbital of Pr^{3+} ion is considered for hybridization. This may be one of the reasons that both FR and LM models could not account for a high value of nearly 17 K for the antiferromagnetic ordering of praseodymium moments (Neel temperature, T_N) for $PrBa_2Cu_3O_{7-\delta}$.[6,9]

Conclusion

High resolution oxygen K-edge and copper L_{23}-edge X-ray

absorption spectra for $Eu_{0.9-x}Pr_xCa_{0.1}BaSrCu_3O_{7-\delta}$ as a function of Pr^{3+} substitution have been obtained by using a bulk sensitive X-ray fluorescence yield technique. The spectral weight of the pre-edge structure in the oxygen 1s X-ray absorption at 527.5 eV corresponding to oxygen 2p hole states on apical oxygen sites and on Cu(1)O chains is constant with increasing praseodymium substitution. On the other hand, the spectral weight at 528.3 eV corresponding to oxygen 2p hole states situated in the $Cu(2)O_2$ planes decreases systematically, while the spectral weight of the upper Hubbard band at 529.4 eV is found to increase at the cost of hole states in the $Cu(2)O_2$ planes with increasing praseodymium substitution. The analyses of the copper L_3-edge also show that the spectral weight of the high energy shoulder at 932.3 eV corresponding to the hole contents in the CuO_2 layers and CuO_3 ribbons decreases with increasing praseodymium concentration. Both the oxygen K-edge and copper L-edge X-ray absorption spectra for $Eu_{0.9-x}Pr_xCa_{0.1}BaSrCu_3O_{7-\delta}$ clearly demonstrate that the hole states are depleted by the praseodymium substitution, which explains the reduction in the T_c. However, the rate at which the depletion occurs is lower in $Eu_{0.9-x}Pr_xCa_{0.1}BaSrCu_3O_{7-\delta}$ compared to that in $Y_{1-x}Pr_xBa_2Cu_3O_{7-\delta}$ and $Dy_{1-x}Pr_xBa_2Cu_3O_{7-\delta}$. This is due to the partial substitution of Ba^{2+} by Sr^{2+} ions and Eu by Ca^{2+} ions, which induces and creates the holes. Our results give evidence in support of the hole-depletion models based on Pr 4f–O $2p_\pi$ hybridization. Further the anomalous behavior of Pr^{3+} can be well explained if one takes into account the 4f–5d mixing in which the 5d level is low lying and which strongly mixes with the 4f orbital of Pr^{3+} ions unlike those of other rare earth metal ions.

References

1 Z. Fisk, J. D. Thompson, E. Zirngiebl, J. L. Smith and S. W. Cheong, *Solid State Commun.*, 1987, **62**, 743.
2 P. H. Hor, R. L. Meng, Y. Q. Wang, L. Gao, Z. J. Huang, J. Bechtold, K. Forster and C. W. Chu, *Phys. Rev. Lett.*, 1987, **58**, 1891.
3 H. B. Radousky, *Mater. Res. Bull.*, 1992, **7**, 1917.
4 J. M. Chen, R. S. Liu, J. G. Lin, C. Y. Huang and J. C. Ho, *Phys. Rev. B*, 1997, **55**, 14586 and refs. therein.
5 R. S. Liu, C. Y. Cheng and J. M. Chen, *Inorg. Chem.*, 1998, **37**, 5527.
6 V. P. S. Awana, S. X. Dou, R. Singh, A. V. Narlikar, S. K. Malik and W. B. Yelon, *J. Appl. Phys.*, 1998, **83**, 7315 and refs. therein.
7 M. Merz, N. Nucker, E. Pellegrin, P. Schweiss, S. Schuppler, M. Kielwein, M. Knupfer, M. S. Golden, J. Fink, C. T. Chen, V. Chakarian, Y. U. Idzerda and A. Erb, *Phys. Rev. B*, 1997, **55**, 9160.
8 M. Merz, N. Nucker, P. Schweiss, S. Schuppler, C. T. Chen, V. Chakarian, J. Freeland, Y. U. Idzerda, M. Klaser, G. Muller-Vogt and Th. Wolf, *Phys. Rev. Lett.*, 1998, **80**, 5192.
9 Y. G. Zhao, Z. W. Dong, M. Rajeswari, R. P. Sharma and T. Venkatesan, *Phys. Rev. B*, 1998, **58**, 1068.
10 H. A. Blackstead and J. D. Dow, *Phys. Rev. B*, 1995, **51**, 11830.
11 Z. Zou, K. Oka, T. Ito and Y. Nishihara, *Jpn. J. Appl. Phys.*, 1997, **36**, L18.
12 Z. Zou, J. Ye, K. Oka and Y. Nishihara, *Phys. Rev. Lett.*, 1998, **80**, 1074.
13 J. Ye, Z. Zou, A. Matsushita, K. Oka, Y. Nishihara and T. Matsumoto, *Phys. Rev. B*, 1998, **58**, R619.
14 D. P. Norton, D. H. Lowndes, B. C. Sales, J. D. Budai, B. C. Chakoumakos and H. R. Kerchner, *Phys. Rev. Lett.*, 1991, **66**, 1537.
15 Y. F. Xiong, Y. S. Yao L. F. Xu, F. Wu, D. Jin and Z. X. Zhao, *Solid State Commun.*, 1998, **107**, 509.
16 A. Matsuda, K. Kinoshita, T. Ishii, H. Shibata, T. Watanabe and T. Yamada, *Phys. Rev. B*, 1988, **38**, 2910.
17 Z. Quirui, Z. H. Zenhui, Z. Han, X. Jiansheng, W. Shenxi and F. Minghu, *Physica C*, 1989, **162**–**164**, 963.
18 B. Fisher, J. Genossar, L. Patlagan and J. Ashkenazi, *Phys. Rev. B*, 1991, **43**, 2821.
19 A. Kebede, C. S. Jee, J. Schwegler, J. E. Crow, T. Mihalisin, G. H. Myer, R. E. Salomon, P. Schlottmann, M. V. Kuric, S. H. Bloom and R. P. Guertin, *Phys. Rev. B*, 1989, **40**, 4517.
20 L. Soderholm, C. K. Loong, G. I. Goodman and B. D. Dabrowski, *Phys. Rev. B*, 1991, **43**, 7923.
21 G. Hilscher, E. Holland-Moritz, T. Holubar, H. D. Jostarndt, V. Nekvasil, G. Schaudy, U. Walter and G. Fillion, *Phys. Rev. B*, 1994, **49**, 535.
22 J. S. Kang, J. W. Allen, Z. X. Shen, W. P. Ellis, J. J. Yeh, B. W. Lee, M. B. Maple, W. E. Speicer and I. Lindau, *J. Less-Common Met.*, 1989, **148**, 121.
23 U. Neukrich, C. T. Simmons, D. Sladeczek, C. Laubschat, O. Strebel, G. Kaindl and D. D. Sarma, *Europhys. Lett.*, 1988, **5**, 567.
24 J. Fink, N. Nucker, H. Romberg, M. Alexander, M. B. Maple, J. J. Neumeier and J. W. Allen, *Phys. Rev. B*, 1990, **42**, 4823.
25 R. Fehrenbacher and T. M. Rice, *Phys. Rev. Lett.*, 1993, **70**, 3471 and refs. therein.
26 A. I. Liechtenstein and I. I. Mazin, *Phys. Rev. Lett.*, 1995, **74**, 1000 and refs. therein.
27 I. K. Gopalakrishnan, T. B. Waje and J. V. Yakhmi, *Physica C*, 1999, **311**, 246.
28 T. B. Waje, Ph.D. Thesis, University of Bombay, 1998.
29 E. H. Appelmann, L. R. Morss, A. M. Kini, U. Geiser, A. Umezawa, G. W. Crabtree and K. D. Carlson, *Inorg. Chem.*, 1987, **26**, 3237.
30 R. D. Shannon, *Acta Crystallogr.*, *Sect. A*, 1976, **32**, 751.
31 T. B. Waje, I. K. Gopalakrishnan and J. V. Yakhmi, *J. Supercond.*, 1998, **10**, 645.
32 P. K. Gallagher, M. M. OBryan, S. A. Sunshine and D. W. Murphy, *Mater. Res. Bull.*, 1987, **22**, 995.
33 J. M. Chen, R. S. Liu, P. Nachimuthu, M. J. Kramer, K. W. Dennis and R. W. McCallum, *Phys. Rev. B*, 1999, **59**, 3855 and refs. therein.
34 H. Krakauer, W. F. Pickett and R. E. Cohen, *J. Supercond.*, 1988, **1**, 111.
35 N. Nucker, E. Pellegrin, P. Schweiss, J. Fink, S. L. Molodtsov, C. T. Simmons, G. Kaindl, W. Frentrup, A. Erb and Muller-Vogt, *Phys. Rev. B*, 1995, **51**, 8529.
36 J. Fink, N. Nucker, E. Pellegrin, H. Romberg, M. Alexander and M. Knupfer, *J. Electron Spectrosc. Relat. Phenom.*, 1994, **66**, 395.
37 J. G. Lin, Y. Y. Xue, C. W. Chu, X. W. Cao and J. C. Ho, *J. Appl. Phys.*, 1993, **73**, 5871.
38 H. Romberg, M. Alexander, N. Nucker, P. Adelmann and J. Fink, *Phys. Rev. B*, 1990, **42**, 8768.
39 C. T. Chen, F. Sette, Y. Ma, M. S. Hybertsen, E. B. Stechel, W. M. C. Foulkes, M. Schluter, S. W. Cheong, A. S. Cooper, L. W. Rupp, Jr., B. Batlogg, Y. L. Soo, Z. H. Ming, A. Krol and Y. H. Kao, *Phys. Rev. Lett.*, 1991, **66**, 104.
40 D. Vaknin, S. K. Shiha, D. E. Moneton, D. C. Johnston, J. M. Newsam, C. R. Safiva and H. E. King, Jr., *Phys. Rev. Lett.*, 1987, **58**, 2802.
41 A. Bianconi, M. De Santis, A. Di Ciccio, A. M. Flank, A. Fronk, A. Fontaine, P. Legarde, H. K. Yoshida, A. Kotani and A. Marcelli, *Phys. Rev. B*, 1988, **38**, 7196.
42 A. Bianconi, M. De Santis, A. Di Ciccio, A. M. Flank, A. Fronk, A. Fontaine, P. Legarde, H. K. Yoshida, A. Kotani and A. Marcelli, *Physica C*, 1988, **153**–**155**, 1760.
43 A. Krol, C. S. Lin, Y. L. Soo, Z. H. Ming, Y. H. Kao, J. H. Wang, M. Qi and G. C. Smith, *Phys. Rev. B*, 1992, **45**, 10051.
44 R. Resifeld and C. K. Jorgensen, *Lasers and Excited States of Rare Earths*, Springer, New York, 1977.
45 R. D. Peacock, *Struct. Bonding* (*Berlin*), 1975, **22**, 83.
46 M. Malinowski, R. Wolski and W. Wolinski, *Solid State Commun.*, 1990, **74**, 17.

Paper 9/02994J